Placed on: Osaka City University Repository

Mem. Fac. Eng., Osaka City Univ., Vol. 38, pp.131—146(1997)

Basic Theory and Numerical Example for Elasto-Plastic and Finite Displacement Analysis of Stiffened Plates with Opening Subjected to Compression

Toshiyuki KITADA*, Yoshiharu IWAI** and Masato KANO***
(Received September 30, 1997)

Synopsis

Described in this paper is a basic theory for elasto-plastic and finite displacement analysis of stiffened plates with the opening subjected to compression in consideration of the initial imperfections such as initial deflection and residual stress on the basis of a finite element method. In this theory, the geometrical nonlinearity caused by the large deflection of plates is formulated according to a total Lagrangian method of removing the rigid body displacement from the global deformation of a finite element, and then the yield condition of von Mises and the plastic flow rule of Prandtl-Reuss with strain hardening are used to simulate elasto-plastic nonlinear behavior of steel material. Unbalanced forces between true nodal forces and applied nodal forces in each step of the iteration calculation are eliminated by the Newton-Raphson's method. A short box column consisting of two mild steel stiffened plates with a circular hole in each of them and two high strength steel flange plates are analyzed as a numerical example. Moreover, these numerical results are compared with the experimental results corresponding to the short box column.

KEYWORDS: elasto-plastic and finite displacement analysis, stiffened plate, opening, compression, numerical example, initial deflection, residual stress

1. Introduction

It is necessary to provide the openings in stiffened plates of steel bridge piers for the sake of fabrication, erection and maintenance of them, despite their constituting stiffened plates subjected to predominant axial compressive forces.

According to the records of disaster by the Hyogo-ken Nambu Earthquake, which occurred in the early morning on January 17, 1995, many highway bridge structures were damaged and collapsed. With regard to the damage of steel bridge piers, the local buckling of stiffened plates in the vicinity of openings located in lower parts of their column members were numerously observed.

In response to these types of damage, first of all, design parameters on the openings in the stiffened plates of steel bridge piers were examined through questionnaires[1]. Secondly, an experimental study on the ultimate strength of stiffened plates with opening was also carried out by using four test models[2]. Then, the elasto-plastic and finite displacement analysis of stiffened plates with opening was performed to investigate their ultimate strength[3].

A basic theory for the elasto-plastic and finite displacement analysis of stiffened plates with opening is described in this paper. The main idea of this theory and the prototype of a computer program USSP (Ultimate Strength of Steel Plated structures) based on this theory was already developed in 1975 by the first author et al[4),5]. Recent improvements for this program are introduced in Ref. 6). The originality of this paper is in a method for introducing the residual stress of stiffened plates with the opening into the finite element models for the analysis of their ultimate strength. The point to be noted is also that this theory is verified through the comparison of numerical results with experimental ones of a short box column consisting of stiffened plates with the opening.

For this analysis, the geometrical nonlinearity caused by the large deflection of plates is formulated according to a total Lagrangian method of removing the rigid body displacement from the global deformation of a finite element, and then the yield condition of von Mises and the plastic flow rule of Prandtl-Reuss with strain hardening are used to simulate elasto-plastic nonlinear behavior of steel material. Unbalanced forces between true nodal forces and applied nodal forces in each step of itera-

* Associate Professor, Department of Civil Engineering
** Student, Doctor Course of Department of Civil Engineering
(Engineering Dept., Steel Structure & Civil Engineering Hq., Mitsui Engineering & Shipbuilding Co., Ltd.)
*** Structural Analysis Division, Bridge and Computer Engineering Co., Ltd.

tion calculation are eliminated by the Newton-Raphson's method. A short box column consisting of two mild steel stiffened plates with a circular hole in each of them and two high strength steel flange plates are analyzed as a numerical example. Moreover, these numerical results are compared with the experimental results corresponding to the short box column.

2. Basic Theory

2.1 Analytical and Numerical Assumptions

The analytical and numerical assumptions of the theory are outlined as follows;

(1) Steel materials to be used are homogeous and isotropic.
(2) The materials behave as perfect elasto-plastic and satisfy the yield condition of von Mises in addition to the plastic flow rule of Prandtl-Reuss.
(3) Displacement of plates and stiffeners follows the Kirchhoff-Love's assumption.
(4) A plate with initial deflection and without any stresses such as residual stress and stress due to applied forces can be approximated as a folded plate assembled with flat triangular finite elements as shown in **Fig.1.**
(5) For a plate with both initial deflection and residual stress simultaneously, the residual stress is introduced into the initial folded plate. Unbalanced forces at the nodal points of the folded plate are caused by introducing the residual stress. They can be, however, eliminated through applying the fictitious nodal forces to the nodal points as illustrated in **Fig.2.**
(6) Each finite element is divided into some layers in order to consider the spread of plastic zone in the direction of thickness. Stress distribution and stiffness in each layer is assumed to vary linearly in the direction of thickness.
(7) Plane stresses in the triangular finite elements are assumed to be constant.
(8) The true nodal forces of the finite elements after their deformation can be calculated on the condition where the non-linear terms in the equations between strains and displacements can be neglected by using the local and net nodal displacements derived by removing rigid body displacements from the global nodal displacements.

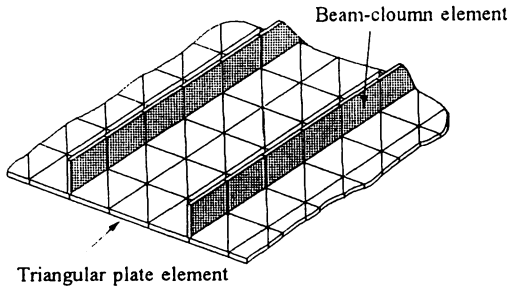

Fig.1 Finite element idealization

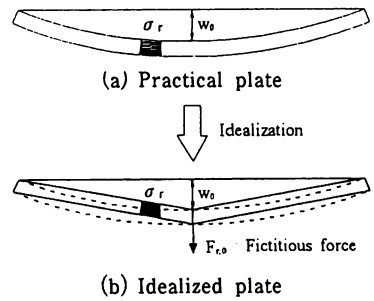

Fig.2 Introduction of residual stress

2.2 Dealing with Geometrical Nonlinearity

Solutions of plate buckling problems concerning the geometrical nonlinearity might be obtained from the formulas relating the nodal force vector to the nodal displacement vector of a finite element model, and containing high order nonlinear terms. However, the formulas are tremendously complicated. For this reason, the geometrical nonlinearity is, hereby, dealt with by extending the Murry-Willson's coordinate movement method[7] on flat plates without initial deflection to flat plates with initial deflection.

An unloaded triangular finite element before the deformation of which apices are i, j and k is shifted onto the deformed triangular finite element of which apices are i', j' and k' in such a method that the node i coincides with the node i', and the side $\overline{ij}$ is laid on the straight line $\overline{i'j'}$ as shown in **Fig.3.** The unloaded triangular finite element after this rigid body movement is defined as the element i"j"k". The displacement of an arbitrary point on the triangular element i'j'k' after the deformation from the corresponding point on the triangular finite element i"j"k" is considered to be net displacement after removing the rigid body displacement. The small displacement theory can be applied for this net displacement by dividing the finite elements as small enough. In this method, the tremendous calculation for deriving the stiffness matrices with high order nonlinear terms can be re-

duced, and then the nonlinearity of material property is only considered in the calculation hereafter.

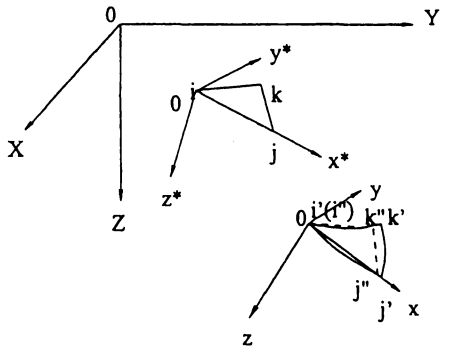

Fig.3 Removal of rigid body displacement

2.3 Formulation of Elasto-Plastic Behavior of Materials

2.3.1 Relationships between stress and strain in a finite element

(1) Plate Elements

The relationship between stress vector σ and strain vector ε is expressed by Eq. (1), where the material remains within elastic range:

$$\sigma = D_e \varepsilon \qquad \text{-----(1)}$$

or

$$\begin{Bmatrix} \sigma_x \\ \sigma_y \\ \tau_{xy} \end{Bmatrix} = \frac{E}{1-\mu^2} \begin{bmatrix} 1 & \mu & 0 \\ \mu & 1 & 0 \\ 0 & 0 & (1-\mu)/2 \end{bmatrix} \begin{Bmatrix} \varepsilon_x \\ \varepsilon_y \\ \gamma_{xy} \end{Bmatrix} \qquad \text{-----(1)'}$$

The relationship between incremental stress vector $\Delta\sigma$ and incremental strain vector $\Delta\varepsilon$ is expressed by Eq. (2) in the elasto-plastic state without considering the strain hardening:

$$\Delta\sigma = D_{ep}\Delta\varepsilon \qquad \text{-----(2)}$$

where D_{ep} is the stress-strain matrix in the elasto-plastic state as shown in below Eq. (10).

Because the incremental strain vector $\Delta\varepsilon$ is separated into the elastic component $\Delta\varepsilon_e$ and the plastic component $\Delta\varepsilon_p$, thus:

$$\Delta\varepsilon = \Delta\varepsilon_e + \Delta\varepsilon_p \qquad \text{----(3)}$$

The elastic incremental strain vector $\Delta\varepsilon_e$ is related to the incremental stress vector $\Delta\sigma$. The elastic incremental strain vetor $\Delta\varepsilon_e$ is, therefore, expressed by:

$$\Delta\varepsilon_e = D_e^{-1}\Delta\sigma \qquad \text{-----(4)}$$

The assumption of the Prandtl-Reuss's plastic flow rule gives the plastic incremental strain vector $\Delta\varepsilon_p$ as follows:

$$\Delta\varepsilon_p = \lambda \left\{ \frac{\partial F}{\partial \sigma} \right\} \qquad \text{----- (5)}$$

where F is the constant to express the yielding condition expressed by Eq. (6) in the case where the material follows the von Mises's yield criteria:

$$F = \sqrt{\sigma_x^2 - \sigma_x\sigma_y + \sigma_y^2 + 3\tau_{xy}^2} - \sigma_Y \qquad \text{-----(6)}$$

where σ_Y is yield stress, and λ designates the possitive coefficient.

From Eqs. (3), (4) and (5), the incremental stress vector $\Delta\sigma$ is expressed by Eq. (7).

$$\Delta\sigma = D_e\left[\Delta\varepsilon - \lambda\left\{\frac{\partial F}{\partial\sigma}\right\}\right] \qquad \text{-----(7)}$$

As the stress vector σ flows on the yield curve in the plastic state, dF is derived by the following equation.

$$dF = \left\{\frac{\partial F}{\partial\sigma}\right\}^T \cdot \Delta\sigma = 0 \qquad \text{-----(8)}$$

After substituting Eq. (7) into Eq. (8), the coefficient λ is given by:

$$\lambda = \frac{\left\{\frac{\partial F}{\partial\sigma}\right\}^T \cdot D_e}{\left\{\frac{\partial F}{\partial\sigma}\right\}^T \cdot D_e \cdot \left\{\frac{\partial F}{\partial\sigma}\right\}} \cdot \Delta\varepsilon \qquad \text{-----(9)}$$

Substituting Eq. (9) into Eq. (7), the stress-strain matrix D_{ep} in the elasto-plastic state is expressed by Eq. (10).

$$D_{ep} = D_e - \frac{D_e \cdot \left\{\frac{\partial F}{\partial\sigma}\right\}\left\{\frac{\partial F}{\partial\sigma}\right\}^T \cdot D_e}{\left\{\frac{\partial F}{\partial\sigma}\right\}^T \cdot D_e \cdot \left\{\frac{\partial F}{\partial\sigma}\right\}} \qquad \text{-----(10)}$$

(2) Stiffener Elements

In the case of stiffener elements, the method to derive the relationship between stress and strain is the same as the plate elements except that the stiffener elements are of one dimension. It means that the stress-strain vector D_e and D_{ep} in Eqs. (1) and (2) are replaced by Young's modulus E and tangent modulus E_t, respectively.

2.3.2 Relationships between incremental displacement and incremental strain in a finite element

(1) Plate elements

Eq. (11) is adopted as the displacement functions to express the in-plane displacements of an arbitrary point p in a triangular finite element shown in **Fig.4.**

$$\left.\begin{aligned}\Delta u &= \alpha_1 + \alpha_2 x + \alpha_3 y\\ \Delta v &= \alpha_4 + \alpha_5 x + \alpha_6 y\end{aligned}\right\} \qquad \text{-----(11)}$$

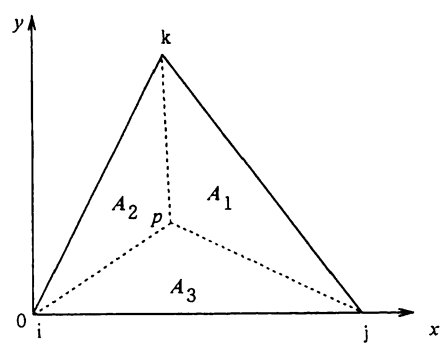

Fig.4 Triangular finite element and element coordinate

The coordinates of the apices i, j and k of the triangular finite element are defined as (x_i, y_i), (x_j, y_j) and (x_k, y_k), respectively. Then, for this element coordinate system, the nodal incremental displacements in the x axial direction are defined as Δu_i, Δu_j and Δu_k, and the nodal incremental displacements in the y axial direction are defined as Δv_i, Δv_j and Δv_k, respectively.

By expressing the incremental displacements, Δu and Δv at an arbitrary point p, in terms of the nodal incremental displacements of the apices of the triangular finite element and by eliminating the coefficients $\alpha_1 \sim \alpha_6$ in Eq. (11), Δu_l is given by:

$$\Delta u_l = N_m \Delta u_{nl} \qquad \text{-----(12)}$$

where Δu_l and N_m are expressed by Eqs. (13) and (14), respectively:

$$\Delta u_l = \left\{ \Delta u,\ \Delta v \right\} \qquad \text{-----(13)}$$

$$N_m = \eta_m\ \zeta_{mn} \qquad \text{-----(14)}$$

where

$$\eta_m = \left\{ 1\ ,\ x,\ y \right\} \qquad \text{-----(15)}$$

Also, ζ_{mn} and Δu_{nl} are given by:

$$\zeta_{mn} = \frac{1}{2A} \begin{pmatrix} x_j y_k - x_k y_j & x_k y_i - x_i y_k & x_i y_j - x_j y_i \\ y_j - y_k & y_k - y_i & y_i - y_j \\ x_k - x_j & x_i - x_k & x_j - x_i \end{pmatrix} \qquad \text{-----(16)}$$

$$\Delta u_{nl} = \begin{pmatrix} \Delta u_i & \Delta v_i \\ \Delta u_j & \Delta v_j \\ \Delta u_k & \Delta v_k \end{pmatrix} \qquad \text{-----(17)}$$

Eq. (18) is obtained by differentiating Eq. (12) partially by x and y:

$$\Delta \varepsilon_l = B_u\ \Delta d_s \qquad \text{-----(18)}$$

where $\Delta \varepsilon_l$, B_u and the nodal incremental displacement vector of the finite element d_s are given by Eqs. (19), (20) and (21), respectively:

$$\Delta \varepsilon_l = \begin{pmatrix} \dfrac{\partial \Delta u}{\partial x} \\ \dfrac{\partial \Delta v}{\partial y} \\ \dfrac{\partial \Delta u}{\partial y} + \dfrac{\partial \Delta v}{\partial x} \end{pmatrix} \qquad \text{-----(19)}$$

$$B_u = \frac{1}{2A} \begin{pmatrix} y_j - y_k & 0 & y_k - y_i & 0 & y_i - y_j & 0 \\ 0 & x_k - x_j & 0 & x_i - x_k & 0 & x_j - x_i \\ x_k - x_j & y_j - y_k & x_i - x_k & y_k - y_i & x_j - x_i & y_i - y_j \end{pmatrix} \qquad \text{-----(20)}$$

$$\Delta d_s = \left\{ \Delta u_i,\ \Delta v_i,\ \Delta u_j,\ \Delta v_j,\ \Delta u_k,\ \Delta v_k \right\}^T \qquad \text{-----(21)}$$

Next, Eq. (22) is adopted as the displacement function to express the out-of-plane displacement of an arbitrary point p in the triangular finite element.

$$\begin{aligned} \Delta w = {} & \alpha_{b1} + \alpha_{b2} L_1 + \alpha_{b3} L_2 + \alpha_{b4} L_1 L_2 + \alpha_{b5} L_2 L_3 + \alpha_{b6} L_3 L_1 \\ & + \alpha_{b7}(L_1 L_2^2 - L_1^2 L_2) + \alpha_{b8}(L_2 L_3^2 - L_2^2 L_3) + \alpha_{b9}(L_3 L_1^2 - L_3^2 L_1) \end{aligned} \qquad \text{-----(22)}$$

Alternatively, Eq. (22) can be expressed in the matrix form as follows:

$$\Delta w = G^T\ \beta \qquad \text{-----(23)}$$

where G^T and β are given by Eqs. (24) and (25), respectively:

$$G^T = \left\{ 1, L_1, L_2, L_1 L_2, L_2 L_3, L_3 L_1, L_1 L_2^2 - L_1^2 L_2, L_2 L_3^2 - L_2^2 L_3, L_3 L_1^2 - L_3^2 L_1 \right\} \qquad \text{-----(24)}$$

$$\beta = \left\{ \alpha_{b1}, \alpha_{b2}, \alpha_{b3}, \alpha_{b4}, \alpha_{b5}, \alpha_{b6}, \alpha_{b7}, \alpha_{b8}, \alpha_{b9} \right\}^T \qquad \text{-----(25)}$$

in which L_1, L_2 and L_3 are the area coordinates. As is shown in Fig. 4, the coordinates of the arbitrary point p in the triangular finite element are (x, y), and each area of the sub-triangles which are formed by connecting the point p with the apices of the triangular finite element is A_1, A_2 and A_3, respectively. Then, the area coordinates are defined as $L_1=A_1/A$, $L_2=A_2/A$ and $L_3=A_3/A$, where A is the area of the finite element. From $L_1+L_2+L_3=1$, the unknown coordinates are reduced into L_1 and L_2. The rectangular coordinates (x, y) of the point p are related to the area coordinates L_1 and L_2 as shown in Eq. (26).

$$\begin{Bmatrix} x \\ y \end{Bmatrix} = \begin{bmatrix} x_i-x_k & x_j-x_k \\ y_i-y_k & y_j-y_k \end{bmatrix} \begin{Bmatrix} L_1 \\ L_2 \end{Bmatrix} + \begin{Bmatrix} x_k \\ y_k \end{Bmatrix} \qquad \text{-----(26)}$$

By using Eq. (26), the partial differential operator with respect to the rectangular coordinates is transformed with the Jacobian matrix J into the partial differential operator with respect to the area coordinates as follows:

$$\begin{Bmatrix} \dfrac{\partial}{\partial x} \\ \dfrac{\partial}{\partial y} \end{Bmatrix} = J \begin{Bmatrix} \dfrac{\partial}{\partial L_1} \\ \dfrac{\partial}{\partial L_2} \end{Bmatrix} \qquad \text{-----(27)}$$

Differentiation of both the sides of Eq. (27) partially by x and y yields the following Eq. (28):

$$\begin{Bmatrix} \dfrac{\partial^2}{\partial x^2} \\ \dfrac{\partial^2}{\partial y^2} \\ \dfrac{\partial^2}{\partial x \partial y} \end{Bmatrix} = T_L \begin{Bmatrix} \dfrac{\partial^2}{\partial L_1^2} \\ \dfrac{\partial^2}{\partial L_2^2} \\ \dfrac{\partial^2}{\partial L_1 \partial L_2} \end{Bmatrix} \qquad \text{-----(28)}$$

where J is given by:

$$J=\frac{1}{2A} \begin{bmatrix} y_j-y_k & y_k-y_i \\ x_k-x_j & x_i-x_k \end{bmatrix} \qquad \text{-----(29)}$$

Moreover, T_L is given by:

$$T_L=\frac{1}{4A^2} \begin{bmatrix} (y_j-y_k)^2 & (y_k-y_i)^2 & 2(y_j-y_k)\ (y_k-y_i) \\ (x_k-x_j)^2 & (x_i-x_k)^2 & 2(x_k-x_j)\ (x_i-x_k) \\ 2(y_j-y_k)(x_k-x_j) & 2(y_k-y_i)(x_i-x_k) & 2\{(y_j-y_k)(x_i-x_k)+(y_k-y_i)(x_k-x_j)\} \end{bmatrix} \qquad \text{-----(30)}$$

Eq. (27) can be transformed into Eq. (31):

$$\begin{Bmatrix} -\dfrac{\partial}{\partial L_2} \\ \dfrac{\partial}{\partial L_1} \end{Bmatrix} = J' \begin{Bmatrix} -\dfrac{\partial}{\partial y} \\ \dfrac{\partial}{\partial x} \end{Bmatrix} \qquad \text{-----(31)}$$

where J' is given by Eq. (32).

$$J' = \begin{bmatrix} y_j-y_k & x_k-x_j \\ y_k-y_i & x_i-x_k \end{bmatrix} \qquad \text{-----(32)}$$

The out-of-plane component $\Delta \boldsymbol{d}_{bLI}$ of the nodal incremental displacement vector $\Delta \boldsymbol{d}_I$ is defined as Eq. (33) with respect to the area coordinate system.

$$\Delta \boldsymbol{d}_{bLI} = \{\Delta w_i,\ -\frac{\partial \Delta w_i}{\partial L_2},\ \frac{\partial \Delta w_i}{\partial L_1},\ \Delta w_j,\ -\frac{\partial \Delta w_j}{\partial L_2},\ \frac{\partial \Delta w_j}{\partial L_1},$$
$$\Delta w_k,\ -\frac{\partial \Delta w_k}{\partial L_2},\ \frac{\partial \Delta w_k}{\partial L_1}\}^T \qquad \text{-----(33)}$$

Eq. (33) is transformed into the out-of-plane component of the nodel incremental displacement vector $\Delta \boldsymbol{d}_{bI}$ with respect to the rectangular coordinate system by Eq. (34):

$$\Delta \boldsymbol{d}_{bLI} = L_j \Delta \boldsymbol{d}_{bI} \qquad \text{-----(34)}$$

where L_j is given by:

$$L_j = \begin{pmatrix} J'' & & 0 \\ & J'' & \\ 0 & & J' \end{pmatrix}, \qquad J'' = \begin{bmatrix} 1 & 0 \\ 0 & J' \end{bmatrix} \qquad \text{-----(35), (36)}$$

Differentiating Eq. (23) partially by L_1 and L_2 and calculating the inverse matrix, the coefficient matrix β in Eq. (23) can be expressed in terms of $\Delta \boldsymbol{d}_{bLI}$ or $\Delta \boldsymbol{d}_{bI}$ as follows:

$$\beta = A_L^{-1} \Delta \boldsymbol{d}_{bLI} = A_L^{-1} L_j \Delta \boldsymbol{d}_{bI} \qquad \text{-----(37)}$$

where A_L^{-1} is given by:

$$A_L^{-1} = \begin{pmatrix} 0 & 0 & 0 & 0 & 0 & 0 & 1 & 0 & 0 \\ 1 & 0 & 0 & 0 & 0 & 0 & -1 & 0 & 0 \\ 0 & 0 & 0 & 1 & 0 & 0 & -1 & 0 & 0 \\ 0 & -1/2 & -1/2 & 0 & 1/2 & 1/2 & 0 & 0 & 0 \\ 0 & 0 & 0 & 0 & 1/2 & 0 & 0 & -1/2 & 0 \\ 0 & 0 & -1/2 & 0 & 0 & 0 & 0 & 0 & 1/2 \\ -1 & 1/2 & 1/2 & 1 & 1/2 & 1/2 & 0 & 0 & 0 \\ 0 & 0 & 0 & -1 & -1/2 & 0 & 1 & -1/2 & 0 \\ 1 & 0 & -1/2 & 0 & 0 & 0 & -1 & 0 & -1/2 \end{pmatrix} \qquad \text{-----(38)}$$

Substitution of Eq. (37) into Eq. (23) yields Eq. (39) which is related Δw to $\Delta \boldsymbol{d}_{bI}$.

$$\Delta w = G^T A_L^{-1} L_j \Delta \boldsymbol{d}_{bI} \qquad \text{-----(39)}$$

If ${G_{L1}}^T$ and ${G_{L2}}^T$ are defined as the area coordinate vectors obtained by differentiating G^T partially by L_1 and L_2, the incremental vector of rotation angle $\Delta \Theta_I$ is given by Eq. (40):

$$\Delta \Theta_I = A_\theta \Delta \boldsymbol{d}_{bI} \qquad \text{-----(40)}$$

where $\Delta \Theta_I$ and A_θ are given by Eqs. (41) and (42), respectively:

$$\Delta \Theta_I = \begin{Bmatrix} \dfrac{\partial \Delta w}{\partial x} \\ \dfrac{\partial \Delta w}{\partial y} \end{Bmatrix} \qquad \text{-----(41)}$$

$$A_\theta = J G_L A_L^{-1} L_j \qquad \text{-----(42)}$$

$$G_L=\begin{Bmatrix} G_{L1}{}^T \\ G_{L2}{}^T \end{Bmatrix} \qquad \text{-----(43)}$$

Moreover, the area coordinate vectors $G_{L11}{}^T$ and $G_{L22}{}^T$ can be derived by differentiaing partially G^T two times with respect to L_1 and L_2, and then the incremental curvature vector $\Delta\Phi_I$ is given by Eq. (44):

$$\Delta\Phi_I=A_\Phi\,\Delta d_{bI} \qquad \text{-----(44)}$$

where $\Delta\Phi_I$ and A_Φ are given by:

$$\Delta\Phi_I=\begin{Bmatrix} \dfrac{\partial^2\Delta w}{\partial x^2} \\ \dfrac{\partial^2\Delta w}{\partial y^2} \\ 2\dfrac{\partial^2\Delta w}{\partial x\partial y} \end{Bmatrix} \qquad \text{-----(45)}$$

$$A_\Phi=T_L P_L A_L{}^{-1} L_j \qquad \text{-----(46)}$$

$$P_L=\begin{Bmatrix} G_{L11}{}^T \\ G_{L22}{}^T \\ G_{L12}{}^T \end{Bmatrix} \qquad \text{-----(47)}$$

By using the incremental in-plane strain vector $\Delta\varepsilon_I$ in the middle surface of the finite element, the incremental rotation angle vector $\Delta\Theta_I$ and the incremental curvature vector $\Delta\Phi_I$ expressed in Eqs. (18), (40) and (44), respectively, the relationship between the incremental strain vector $\Delta\varepsilon_I$ and the nodal incremental displacement vectors Δd_{sI} and Δd_{bI} at an arbitrary point in the finite element is given by Eq. (48):

$$\Delta\varepsilon_I=B_u\cdot\Delta d_{sI}+1/2\cdot\Delta C_{\theta I}\cdot A_\theta\cdot\Delta d_{bI}+C_{\theta I}\cdot A_\theta\cdot\Delta d_{bI}-z\cdot A_\Phi\cdot\Delta d_{bI} \qquad \text{-----(48)}$$

where $C_{\theta I}$ and $\Delta C_{\theta I}$ are given by Eqs. (49) and (50), respectively:

$$C_{\theta I}=\begin{pmatrix} \dfrac{\partial w_0}{\partial x} & 0 \\ 0 & \dfrac{\partial w_0}{\partial y} \\ \dfrac{\partial w_0}{\partial y} & \dfrac{\partial w_0}{\partial x} \end{pmatrix} \qquad \Delta C_{\theta I}=\begin{pmatrix} \dfrac{\partial\Delta w}{\partial x} & 0 \\ 0 & \dfrac{\partial\Delta w}{\partial y} \\ \dfrac{\partial\Delta w}{\partial y} & \dfrac{\partial\Delta w}{\partial x} \end{pmatrix} \qquad \text{-----(49), (50)}$$

(2) Stiffener Elements

The relationship between the nodal incremental displacement vector and the incremental strain vector in a stiffener element is obtained in the similar manner to the plate elements. Consequently, the equation relating the incremental strain vector $\Delta\varepsilon_R$ at an arbitrary point in the stiffener element to the incremental displacement vector in the axial direction Δd_{Rn} and the incremental displacement vector of flexure Δd_{Rb} is given by Eq. (51):

$$\Delta\varepsilon_R=B_{Rn}\cdot\Delta d_{Rn}-z\cdot B_{Rb}\cdot\Delta d_{Rb} \qquad \text{-----(51)}$$

where B_{Rn}, Δd_{Rn}, B_{Rb} and d_{Rb} are given by:

$$B_{Rn}=[-1/L,\ 1/L] \qquad \text{-----(52)}$$

$$\Delta \boldsymbol{d}_{Rn}=\{\Delta u_{Ri},\ \Delta u_{Rj}\}^{T} \qquad \text{-----(53)}$$

$$\boldsymbol{B}_{Rb}=[2\ \ 6x]\begin{bmatrix} -3/L^2 & -2/L & 3/L^2 & -1/L \\ 2/L^3 & 1/L^2 & -2/L^3 & 1/L^2 \end{bmatrix} \qquad \text{-----(54)}$$

$$\boldsymbol{d}_{Rb}=\begin{Bmatrix} \Delta w_{Ri} \\ \dfrac{\partial \Delta w_{Ri}}{\partial x} \\ \Delta w_{Rj} \\ \dfrac{\partial \Delta w_{Rj}}{\partial x} \end{Bmatrix} \qquad \text{-----(55)}$$

Fig.5 Stiffener element

in which L is the length of the stiffener element, and Δu_i, Δu_j, Δw_i and Δw_j are the displacements in the axial direction and the deflections at the nodal points i and j as shown in **Fig.5.**

2.3.3 Equations of equilibrium

A structure idealized by an assembly of finite elements is in a state after I-th iteration from an equilibrium state M (the iteration state I) where the nodal force vector $\boldsymbol{f}_I$ induces the internal stress vector σ_I in a finite element. In the next loading step (step I) that the internal stress vector is increased by $\Delta\sigma_I$ by the nodal force vector increased by $\Delta\boldsymbol{f}_I$ in the finite element, the equation of equilibrium condition of the finite element can be obtained according to the principle of virtual work. Therefore, Eq. (56) is valid by using the virtual nodal displacement vector $\delta\boldsymbol{d}$ and the virtual strain vector $\delta\varepsilon$.

$$\int \delta\varepsilon^{T}(\sigma_I+\Delta\sigma_I)\,dV=\delta\boldsymbol{d}^{T}(\boldsymbol{f}_I+\Delta\boldsymbol{f}_I) \qquad \text{-----(56)}$$

Substitution of Eqs. (2) and (48) into Eq. (56) gives:

$$\boldsymbol{f}_I+\Delta\boldsymbol{f}_I=\begin{Bmatrix} \boldsymbol{f}_{sI} \\ \boldsymbol{f}_{bI}+\int A_\theta{}^{T}C_\theta{}^{T}\sigma_I dV \end{Bmatrix}+\begin{bmatrix} \boldsymbol{k}_{ssI} & \int B_u{}^{T}D_I C_{\theta I} A_\theta\,dV+\boldsymbol{k}_{sbI} \\ \int A_\theta{}^{T}C_{\theta I}{}^{T}D_I B_u\,dV+\boldsymbol{k}_{bsI} & \boldsymbol{k}_{BBI} \end{bmatrix}\begin{Bmatrix} \Delta\boldsymbol{d}_{sI} \\ \Delta\boldsymbol{d}_{bI} \end{Bmatrix}$$

$$\text{----(57)}$$

where $\boldsymbol{f}_{sI}$, $\boldsymbol{f}_{bI}$, $\boldsymbol{k}_{ssI}$, $\boldsymbol{k}_{sbI}$ and $\boldsymbol{k}_{BBI}$ are given by:

$$\left.\begin{aligned} &\boldsymbol{f}_{sI}=\int B_u{}^{T}\cdot\sigma_I\cdot dV, \quad \boldsymbol{f}_{bI}=-\int z\cdot A_\Phi{}^{T}\cdot\sigma_I\cdot dV \\ &\boldsymbol{k}_{ssI}=\int B_u{}^{T}\cdot D_I\cdot B_u\cdot dV, \quad \boldsymbol{k}_{sbI}=\boldsymbol{k}_{bsI}{}^{T}=-\int z\cdot B_u{}^{T}\cdot D_I\cdot A_\Phi\cdot dV \end{aligned}\right\}\ \text{----(58)}\sim(61)$$

$$\boldsymbol{k}_{BBI}=\boldsymbol{k}_{bbI}+\boldsymbol{k}_{GI}+\int A_\theta{}^{T}\cdot C_{\theta I}{}^{T}\cdot D_I\cdot C_{\theta I}\cdot A_\theta\cdot dV-\int z\cdot A_\theta{}^{T}\cdot C_{\theta I}{}^{T}\cdot D_I\cdot A_\theta\cdot dV$$
$$-\int z\cdot A_\theta{}^{T}\cdot D_I\cdot C_{\theta I}\cdot A_\theta\cdot dV \qquad \text{---(62)}$$

$$\boldsymbol{k}_{bbI}=\int z^2\cdot A_\Phi{}^{T}\cdot D_I\cdot A_\Phi\cdot dV, \quad \boldsymbol{k}_{GI}=\int A_\theta{}^{T}\cdot P_I\cdot A_\theta\cdot dV \qquad \text{----(63), (64)}$$

$$P_I=\begin{bmatrix} \sigma_x & \tau_{xy} \\ \tau_{xy} & \sigma_y \end{bmatrix} \qquad \text{----(65)}$$

If the size of the finite elements is so small that the error of the numerical results can practically be ignored, the deformed structure at the iteration state I before the loading step I can be also approximated by the assembly of flat plate finite elements. Therefore, Eqs. (66) and (67) are held by the following conditions:

$$\frac{\partial w_o}{\partial x}=0, \quad \frac{\partial w_o}{\partial y}=0 \qquad \text{----(66), (67)}$$

Hence $C_{\theta I}=0$ from Eq. (49), then Eq. (57) is simplified into Eq. (68).

$$\Delta f_I=\begin{bmatrix} k_{ssI} & k_{sbI} \\ k_{bsI} & k_{bbI}+k_{GI} \end{bmatrix}\cdot\begin{bmatrix} \Delta d_{sI} \\ \Delta d_{bI} \end{bmatrix}=k_I\cdot\Delta d_I \qquad \text{-----(68)}$$

where k_I is the tangent stiffness matrix of the flat plate element. The tangent stiffness matrix of a stiffener element can be derived in the similar manner. After transforming these tangent stiffness matrices with respect to the element coordinate system into the global coordinate system and assembling all the tangent stiffness matrices, the global equilibrium equation of the structure with the global tangent stiffness matrix is given by Eq. (69).

$$\Delta F_I = K_I\cdot\Delta U_I \qquad \text{-----(69)}$$

The incremental displacement vector ΔU_I corresponding to the incremental applied load vector ΔF_I is obtained by solving Eq. (69) after modifying them by the boundary conditions.

2.4 Formulation of Unbalanced Forces

In the iteration state I after the I-th time iteration of calculation by using Eq. (69) from the equilibrium state M, the stress vector σ_I and strain vector ε_I in a finite element are given by Eqs. (70) and (71) as shown in **Fig.6**:

$$\sigma_I=\sigma_M+\Delta\sigma_M \qquad \text{-----(70)}$$

$$\varepsilon_I=\varepsilon_M+\Delta\varepsilon_M \qquad \text{------(71)}$$

where σ_M and ε_M are stress and strain vectors at the equilibrium state M, respectively, and means incremental vector from the equilibrium state M.

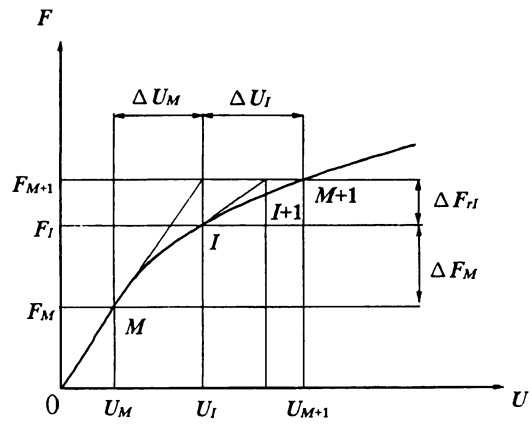

Fig.6 Load vector F — displacement vector U curve

Considering Eq. (2), σ_I is given by:

$$\sigma_I=\sigma_M+D_M\Delta\varepsilon_M \qquad \text{------(72)}$$

where

$$D_M=\begin{cases} D_e & \text{(elastic or strain reversal)} \\ \alpha D_e+(1-\alpha)D_{ep} & \text{(transition from elastic into plastic)} \\ D_{ep} & \text{(plastic)} \end{cases} \qquad \text{------(73)}$$

For a finite element which was elastic in the equilibrium state M, but have changed to be plastic in the iteration state I, the incremental strain vector is separated into the plastic and the elastic ranges. The parameter α is the ratio of the incremental strain vector up to just the yielding to the total incremental strain vector, being decided by the following equation.

$$(\sigma_{xM}+\alpha\cdot\Delta\sigma_{xM})^2-(\sigma_{xM}+\alpha\cdot\Delta\sigma_{xM})\cdot(\sigma_{yM}+\alpha\cdot\Delta\sigma_{yM})$$
$$+(\sigma_{yM}+\alpha\cdot\Delta\sigma_{yM})^2+3(\tau_{xyM}+\alpha\cdot\Delta\tau_{xyM})^2=\sigma_Y^2 \qquad \text{------(74)}$$

For the net nodal incremental displacement vector $\Delta\boldsymbol{u}_M$ which is the nodal incremental vector removed the rigid body displacement vector through the method as mentioned in 2.2, the small displacement theory can be adopted. The relationship between the incremental strain vector $\Delta\boldsymbol{\varepsilon}_M$ and the net nodal incremental displacement vector $\Delta\boldsymbol{u}_M$ is, therefore, given by Eq. (75):

$$\Delta\boldsymbol{\varepsilon}_M=\boldsymbol{\varepsilon}_I-\boldsymbol{\varepsilon}_M=A\cdot\Delta\boldsymbol{u}_M \qquad \text{------(75)}$$

where A is expressed by:

$$A=[B_u,\ -z\cdot A_\phi] \qquad \text{------(76)}$$

By the principle of virtual work, Eq. (77) is held by using the virtual strain vector $\delta\boldsymbol{\varepsilon}$ and the virtual nodal displacement vector $\delta\boldsymbol{u}$.

$$\int\delta\boldsymbol{\varepsilon}^{\mathrm{T}}\sigma_I dV=\delta\boldsymbol{u}^{\mathrm{T}}f_I \qquad \text{------(77)}$$

Substituting Eqs. (72) and (75) into Eq. (77), and considering that Eq. (77) must be valid for arbitrary $\delta\boldsymbol{u}$, Eq. (78) can be obtained as follows:

$$f_I=f_M+k_M\cdot\Delta\boldsymbol{u}_M \qquad \text{------(78)}$$

where f_M and k_M are expressed by Eqs. (79) and (80), respectively:

$$f_M=\int A^{\mathrm{T}}\cdot\sigma_M dV \qquad \text{------(79)}$$

$$k_M=\int A^{\mathrm{T}}\cdot D_M\cdot A dV \qquad \text{------(80)}$$

From Eq. (78), the nodal incremental force vector of each finite element is given by:

$$\Delta f_M=k_M\cdot\Delta\boldsymbol{u}_M \qquad \text{------(81)}$$

The true nodal force vector f_I in the iteration stage I is obtained through adding Δf_M to the true nodal force vector f_M in the equilibrium state M. The true nodal force vector F_I in the global structure is obtained through transforming f_I with respect to the element coordinate system into the true nodal force vector with respect to the global coordinate system and assembling them together with the true nodal force vectors of the other finite elements. Thus, the unbalanced force vector ΔF_{rI} is given by the Eq. (82):

$$\Delta F_{rI}=F_{(M+1)}-F_I \qquad \text{------(82)}$$

where $F_{(M+1)}$ is the nodal applied force vector in the global structure.

3. Method for Introducing Residual Stress into Finite Element Models

Residual stress is one of the inevitable factors which affect adverse influence upon the ultimate strength of stiffened plates with the opening.

Fig.7 shows the idealized distributions of the residual stress to be used in the elasto-plastic and finte displacement analysis for stiffened plates with the opening strengthened by a doubler plate or not strengthened. They are assumed on the basis of measured distributions of residual stress [3]. The residual stress distribution (Type A) caused by gas-arc cutting can be idealized as shown in Fig. 7(a). The residual stress distribution (Type B) in a doubler plate is caused by welding them

onto a plate with the opening and can be idealized as shown in Fig. 7 (b). The residual stress distribution (Type C) in a plate with the opening, which is caused by welding a doubler plate onto them, can be idealized as shown in Fig. 7 (c). The idealized longitudinal residual stress distributions (Type D) in stiffened plates and stiffeners, and idealized transverse residual stress distribution (Type E) caused by welding of transverse stiffeners are also depicted in Figs. 7 (d) and (e).

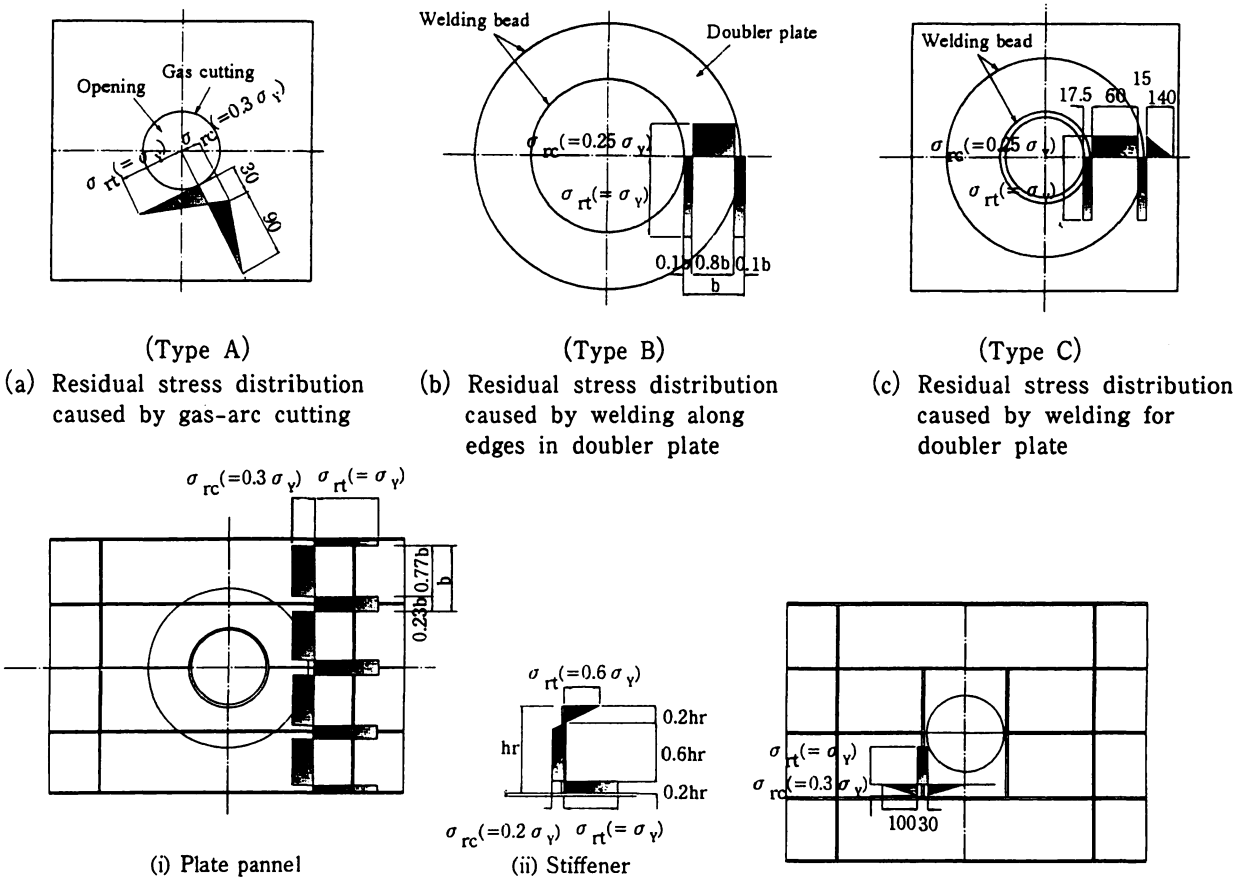

(Type A)
(a) Residual stress distribution caused by gas-arc cutting

(Type B)
(b) Residual stress distribution caused by welding along edges in doubler plate

(Type C)
(c) Residual stress distribution caused by welding for doubler plate

(i) Plate pannel
(ii) Stiffener
(Type D)
(d) Longitudinal residual stress distribution caused by welding for longitudinal stiffeners

(Type E)
(e) Transverse residual stress distribution caused by welding for transverse stiffeners

Fig. 7 Idealized distributions of residual stresses for analysis (dimensions in mm)[3)]

The residual stress distribution of a stiffened plate with the opening under consideration can be approximately generated in the finite element model by superposing properly some or all of the types of the distributions shown in Fig. 7 as follows;

(i) The residual stress distributions of Types A, B and C are assumed to be constant in the direction along the circumference of the hole. Therefore, the residual stress distribution along an arbitrary radial direction can be obtained by rotating the residual stress distributions shown in Fig. 7 about the center of the hole .

(ii) The residual stress distributions of Types D and E are assumed to be constant in the longitudinal and transverse directions, respectively.

(iii) The residual stress Type A can be supposed to be absorbed in the residual stress distribution Type C in case that the doubler plate is welded.

(iv) All the types of the residual stress distributions to be necessary for a stiffened plate with the opening under consideration are superposed after they are transformed into the residual stresses with respect to the global coordinate system.

(v) The residual stress σ_{rx}, σ_{ry} and τ_{rxy} in each finite element are changed into the equivalent

and constant values.

(vi) In the finite elements where the equivalent stresses $\overline{\sigma}_r$ expressed in Eq. (83) after the superposition exceed the yield stress σ_Y, the components of the residual stresses must be reduced by multiplying them by $\sigma_Y/\overline{\sigma}_r$ in order to make the equivalent stress equal to the yield stress:

$$\overline{\sigma}_r=\sqrt{\sigma_{rx}^2-\sigma_{rx}\sigma_{ry}+\sigma_{ry}^2+3\tau_{rxy}^2} \qquad \text{-----(83)}$$

where σ_{rx}, σ_{ry}, and τ_{rxy} are the residual stresses.

4. Numerical Example

4.1 Analytical Model

The test model No. 2 subjected to uni-axial compression in Ref. 2) is selected as the numerical example. The side elevation and the cross section of the test model are shown in **Fig. 8**. It has a circular hole without any enhancement around them in each one of the two stiffened web plates made of mild steel (SS400), while the two flange plates are made of high strength steel (HT780).

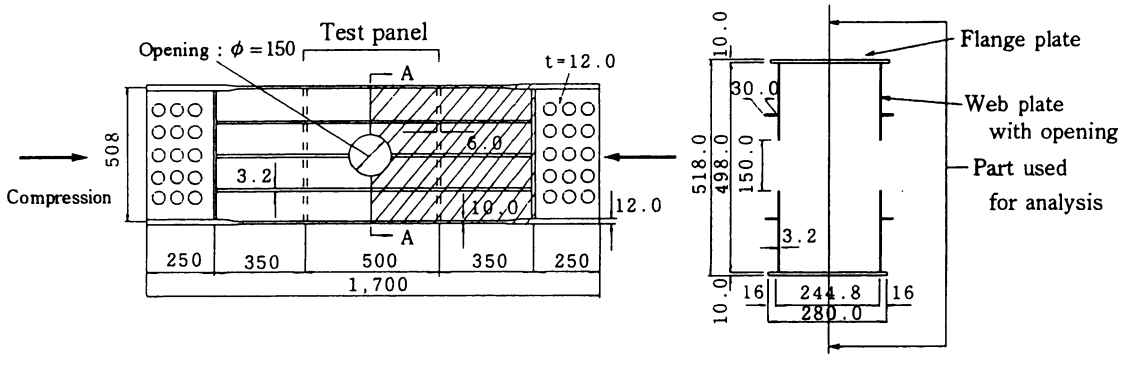

(a) Side elevation (b) Cross section A-A

Fig. 8 Side elevation and cross section of test model No. 2 (dimensions in mm)

The analytical model and the initial deflection curves adopted in this analysis are illustrated in **Fig. 9**.

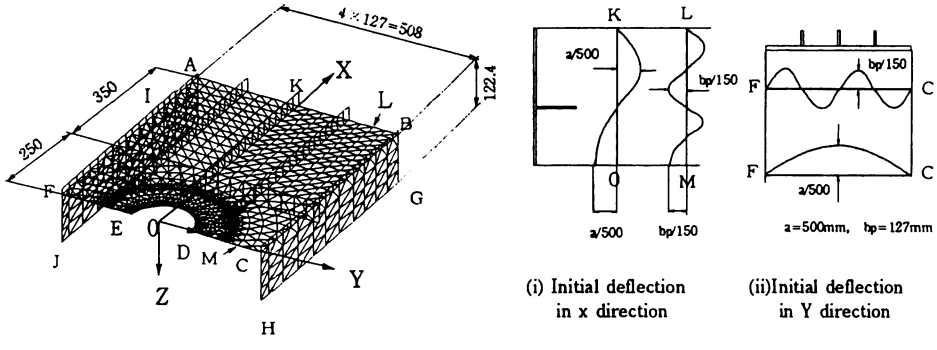

(i) Initial deflection in x direction (ii) Initial deflection in Y direction

(a) Analytical model (b) Initial deflection curves

Fig. 9 Analytical model and initial deflection curves (dimensions in mm)

The analytical model is formed by paying attention to the shaded part of the side elevation of the test model No. 2 in Fig. 8. It corresponds to one fourth model, because of the symmetry on the shape and deflection of the test model No. 2. Proper mesh division of finite element models for stiffened plates with the opening was investigated in Ref. 3). The result is, therefore, adopted in deciding the mesh division of the analytical model shown in Fig. 9. The initial deflection curves are selected on the basis of the measured initial deflection curves in the test model [2].

The residual stress distributions of Types A and D are adopted and are introduced in the similar manner mentioned in Chapter 3.

Fig. 10 shows the residual stress distribution utilized in the analysis compared with the measured residual stresses[3]. They are all non-dimensionalized by the yield stress of the test model. It can be seen from Fig. 10 that the assumed residual stress distribution is agree well with the measured values.

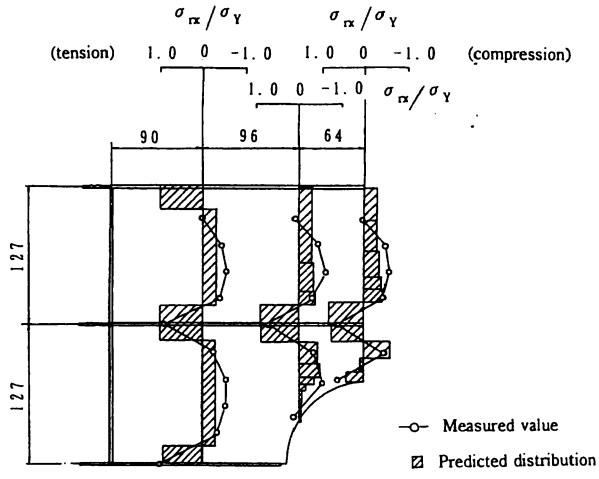

Fig. 10 Residual stress distribution adopted in analysis and measured one (dimension in mm)

Table 1 Boundary conditions (see Fig. 9(a))

Position \ Nodal displacements	u	v	w	θx	θy	θz
Side AB	2	0	1	1	0	1
Side AI, BG	2	1	0	1	1	0
Point A, B	2	1	1	1	1	1
Point G, I	2	1	1	1	1	0
Side GH, IJ	0	0	1	1	1	0
Side CD, EF	1	0	0	0	1	1
Side FJ, CH	1	0	0	0	1	1
Half Circle ED	0	0	0	0	0	1
Point H, J	1	0	1	1	1	1

remarks: 0 = free
1 = constraint
2 = controlled in-plane displacement

The boundary conditions for the analytical model are summarized in **Table 1.** Material properties of the steel plates adopted for the analytical model are listed in **Table 2.**

Table 2 Material properties of web and flange plates

Plates \ Items	Thickness t(cm)	Young's Modulus E(kgf/cm²)	Poisson's Ratio μ	Yield Point σ_Y (kgf/cm²)
Web	0.314	2.17×10^6	0.28	3.472
Flange	1.005	2.16×10^6	0.27	8.573

4.2 Analytical Results

Shown in **Fig. 11** are the situations of spread of plastic zone in three load stages in the vicinity of the ultimate state. In this figure, P_u means the applied axial load to the web plate at the ultimate state, and also $0.60P_u$ means that the applied axial load at the load step is 60% of the ultimate load P_u. It can be seen from Fig. 11 that the plastic zone expands from the outstanding plate parts adjacent to the opening near the center line of the test model to its radial direction.

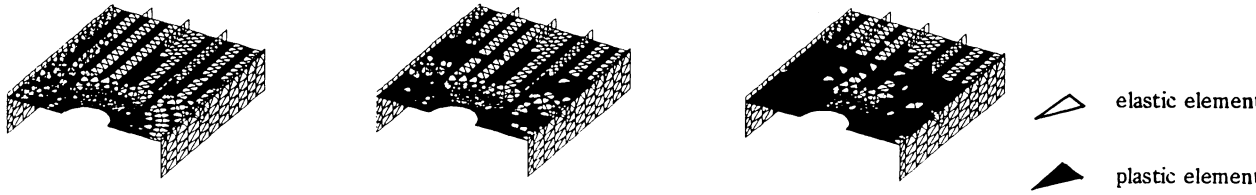

(a) $0.60P_u$ (b) $0.82P_u$ (c) $1.00P_u$

Fig. 11 Spread of plastic zone

The relationships between the longitudinal and in-plane average stress in the web plate and the longitudinal and in-plane strains at an edge point near the circumference of the hole are compared with the experimental results as shown in **Fig. 12.** These values are non-dimensionalized by the yield stress and the yield strain, respectively.

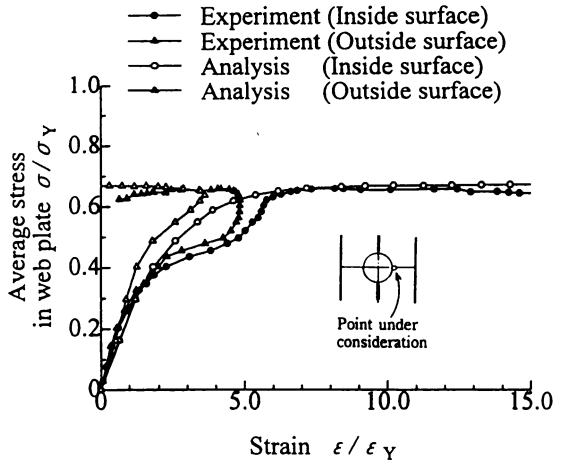

Fig. 12 Relationships between average stress in web plate and strain at edge point

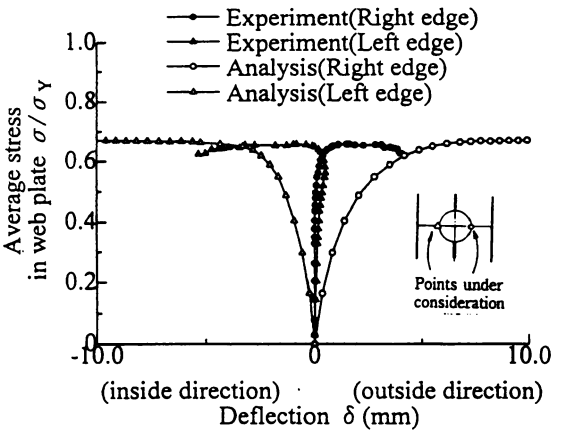

Fig. 13 Relationships between average stress in web plate and deflections at edge points

The analytical relationships between the average stress in the web plate and the deflections at the two side edge points near the circumference are compared with the experimental results in **Fig. 13.** It can be seen from both the analytical and experimental results that the plate edges of the right and left sides of the hole deflect in the outside and inside directions of the box, respectively.

It is considered that the behavior of the strains and deflections of these edge points near the circumference of the hole up to the ultimate state does not agree well quantitatively, but it almost agree qualitatively between the analytical and experimental results, because the local initial deflection near the hole in the analytical model is different from that of the test model. The difference of the local strains and deflections between the analytical and experimental results is considered to affect less influence upon the ultimate strength of stiffened plates with opening and the overall behavior of them up to the ultimate state.

The analytical relationship between the applied axial force to the web plate and the axial displacement is compared with the experimental one as shown in **Fig. 14.** The ordinate of this figure is the applied axial force P divided by the squash load P_Y of the web plate, and the abscissa is the displacement divided by the yielding displacement of the web plate with the opening. Both the analytical and experimental load-displacement curves have almost same tendency. Then, the values of the non-dimensionalized ultimate strength are 0.671 in the analysis, and 0.660 in the experiment. They are situated in good agreement. The slight difference of the axial displacement up to the ultimate state between the analytical and experimental results is considered to be caused by the difference of the residual stress distributions in the analytical and the test models.

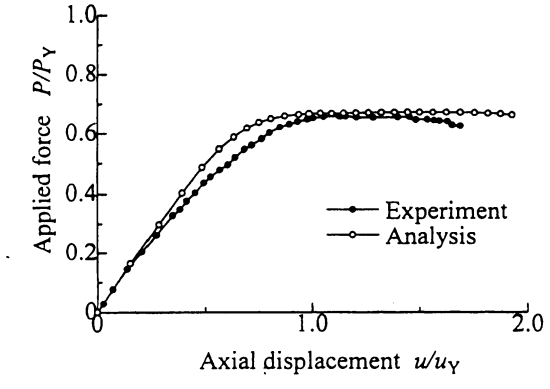

Fig. 14 Relationship between applied axial force to web plate and axial displacement

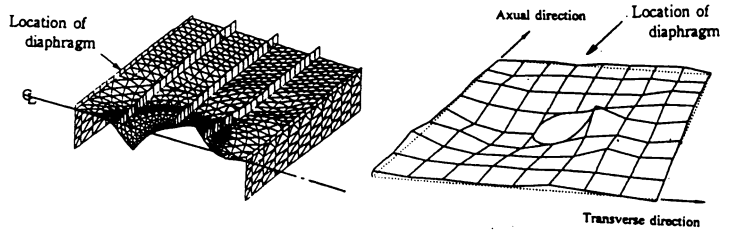

(a) Analysis (b) Experiment

Fig. 15 Deformations of analytical and experimental models at ultimate state

The deformation shapes of the analytical and experimental stiffened plates with the opening at the ultimate state are compared with each other as shown in **Fig. 15**. The deformed shapes of both the analytical and experimental stiffened plates have 3 half waves in the transverse direction, and the shapes of the deformation are well resemble.

5. Conclusion

The main conclusions obtained in this study are summarized as follows:

(1) A basic theory of elasto-plastic and finite displacement analysis of stiffened plates with opening is described on the basis of the finite element method.

(2) One of methods for introducing a proper residual stress distribution into the finite element models for stiffened plates with opening are discussed. It is shown that the residual stress distribution adopted for the analysis is good agreement with the measured one in the corresponding test model.

(3) In the numerical example of the stiffened plate with opening without any enhancement, the analytical results agree well with the experimental ones.

(4) It can be concluded that the behavior up to the ultimate state and the ultimate strength of stiffened plates with opening can be analyzed with good accuracy by the method proposed in this paper.

Acknowelgements

The authors would like to express their much appreciation to Professor Hiroshi Nakai for his valuable advice and suggestion on writing this paper and also to Mr. Toshiro Yamano of Bridge and Computer Engineering Co., Ltd. for assisting the analysis of the numerical example.

References

1) Nakai, H., Kitada, T., Suzuki, I., Horie, Y. and Iwai, Y. : Survey on the Compressive Stiffened Plates with Opening, Bridge and Foundation Engineering, Vol. 30, No. 9, pp. 31-38, September 1996 (in Japanese).

2) Nakai, H., Kitada, T., Iwai, Y., Suzuki, I., Horie, Y. and Mihara, M. : Experimental Study on Ultimate Strength of Stiffened Plates with Opening Subjected to Compressive Force, Proceedings of International Conference on Advances in Steel Structures, Hong Kong, pp. 703-708, December 1996.

3) Nakai, H., Kitada, T., Iwai, Y. and Mihara, M. : On an Elasto-Plastic Finite Displacement Analysis of Stiffened Plates with Opening Subjected to Compression, Proceedings of 4th Japan-Korea Joint Seminar on Steel Bridges, Osaka, Japan, pp. 373-386, December 1996.

4) Komatsu, S., Kitada, T. and Miyazaki, S. : Elasto-Plastic Finite Displacement Analysis of Plates in Compression with Residual Stress and Initial Deflection, Proceedings of Japan Society of Civil Engineers (JSCE), No. 244, pp. 1-14, December 1975 (in Japanese).

5) Komatu, S. and Kitada, T. : Elasto-Plastic Finite Displacement Analysis of Longitudinally Stiffened Plates in Compression, Proceedings of Japan Society of Civil Engineers (JSCE), No. 296, pp. 1-12, April 1980 (in Japanese).

6) Kano, M., Yamano, T., Nibu, M. and Kitada, T. : A Computer Program, USSP, for Analyzing Ultimate Strength of Steel Plated Structures, Proceedings of 5th International Colloquium on Stability and Ductility of Steel Structures, Vol. 2, pp. 763-770, July, 1997.

7) Murray, D. W. and Wilson, E. L. :Finite-Element Postbuckling Analysis of Thin Elastic Plates, American Institute of Aeronautics and Astronautics (AIAA) Journal, Vol. 7, No. 10, pp. 1915-1920, October 1969.